Frequency Coupling Matrix of a Voltage-Source Converter Derived From Piecewise Linear Differential Equations

P. W. Lehn, *Senior Member, IEEE*, and K. L. Lian, *Student Member, IEEE*

***Abstract*—When a power-electronic converter is introduced into a linear network, voltage and current harmonics of differing orders become coupled (through the modulation effect of the converter). The interharmonic coupling introduced by the modulation effect of a converter may be mathematically represented through a frequency coupling matrix (FCM). Given that the source of the coupling is a modulation process, researchers have, in the past, focused on deriving the FCM in the frequency domain—a process that requires the truncation of the harmonic representation of signals. This paper presents an alternate approach to evaluate the FCM based on a time-domain derivation. In contrast to frequency-domain-based methods, it is shown that the time-domain approach avoids truncation. Furthermore, the time-domain approach does not require system linearization about an operating point; thus, the FCM is not limited by small-signal assumptions.**

***Index Terms*—Admittance matrix, frequency coupling matrix (FCM), harmonics, steady-state analysis, voltage-source converter (VSC).**

I. Introduction

THE detrimental effects caused by harmonics include overheating of components, mechanical oscillations in generators and motors, insulation or capacitor failure, and induced interference in communication circuits. It is therefore essential to predict how harmonic sources, such as power-electronic equipment, interact with power systems and to quantify the distortion in voltage and current waveforms at various locations in the power network. Brute-force time-domain simulations can provide accurate harmonic analysis results if the simulation step is chosen appropriately; however, computation times are excessively long when the power network contains switching circuits. Consequently, most harmonic studies are done in the frequency (or harmonic) domain. A detailed summary on frequency-domain analysis can be found in [1]–[3].

In general, most of the frequency-domain algorithms rely on the relation [1], [3]

$$[I] = [Y][V] \qquad \text{or} \qquad [V] = [Y]^{-1}[I] \tag{1}$$

where V is the vector containing voltage harmonics at each node, I is the vector of current harmonics, and Y is the harmonic admittance matrix. To employ the formulation of (1), a harmonic admittance matrix must be found. For linear time invariant (LTI) components such as resistors (R), inductors (L), and capacitors (C), these admittance matrices are easily obtained by phasor analysis. The admittance matrices are diagonal, which means that there is no interaction between harmonic voltages and currents of different orders. For power electronic components, which are linear time varying (LTV), offdiagonal elements exist in the admittance matrix, indicating that voltage and current harmonics with different orders are "cross-coupled" [4]–[7], making the modeling a challenging task.

Previous work dealing with LTV system can be generally classified into two types. The first type is the "transfer function" method [8]–[16]. The transfer function method leads to a model useful for both dynamic and steady-state analysis. However, transfer function methods model only the low-frequency or small-signal behavior of the VSC and they typically neglect switching harmonics as shown in [10]–[12], [14], [15].

The second type of model employs a "harmonic admittance matrix" [4]–[7], also known as the l"frequency coupling matrix" (FCM) [17], [18]. These methods focus on finding the steady-state relation between the voltage and current harmonics of a converter while accounting for the harmonics generated by the converter's switching action.

Typically, the FCM is determined via frequency-domain analysis [3]–[6], [17]–[20] based on the modulation of the converter. The spectra of the switching functions [21] are described as a function of the switching instants [18], [19], as defined by the modulation theory [22]. All converter harmonics are theoretically accounted for in this analysis, however, since the spectra of the switching function are not bandlimited, the computation process requires repeated truncation of harmonic spectra.

The focus of this paper is to determine the FCM via time-domain analysis. The proposed method is compared with existing frequency-domain methods. It is shown that carrying out the analysis in the time domain allows truncation errors to be avoided.

II. Problem of Statement

Advances in the voltage and current ratings of self-commutated semiconductor switches, such as insulated-gate bipolar transistors (IGBTs) and gate turnoff thyristors (GTOs), have resulted in widespread use of VSC throughout the utility network.

Manuscript received January 19, 2006; revised July 27, 2006. Paper no. TPWRD-00020-2006.

The authors are with the Energy System Group, University of Toronto, Toronto, ON M5S 3G4, Canada (e-mail: lehn@ecf.utoronto.ca; liank@ecf.utoronto.ca).

Color versions of one or more of the figures in this paper are available online at http://ieeexplore.ieee.org.

Digital Object Identifier 10.1109/TPWRD.2006.886779

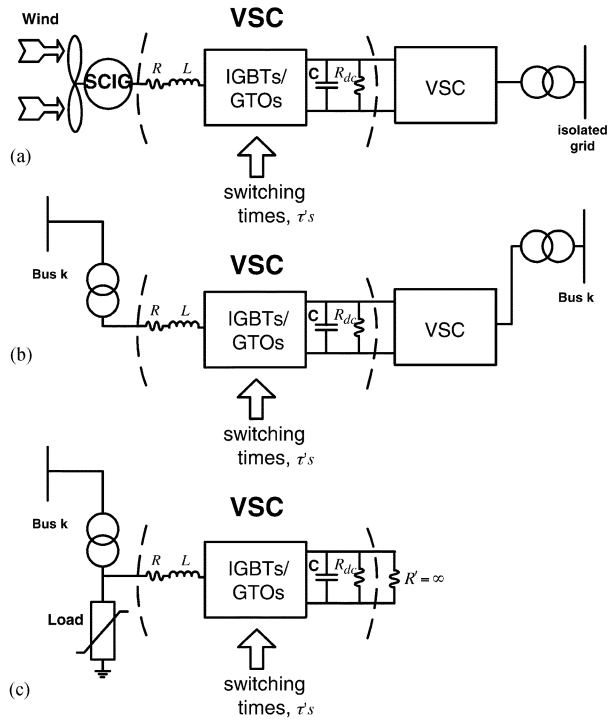

Fig. 1. (a) Generation level: for example, squirrel-cage induction generator (SCIG) wind energy conversion system. (b) Transmission level: for example, UPFC and (c) distribution level, for example, shunt active filter.

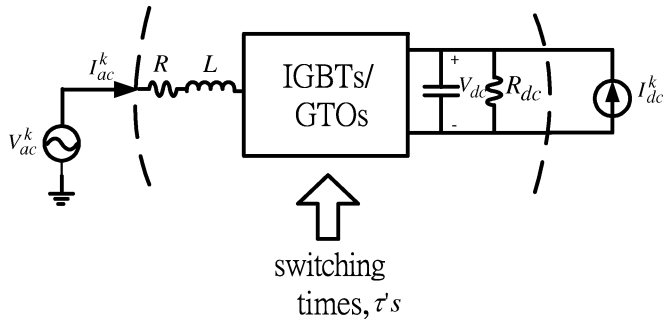

Fig. 2. Equivalent VSC's external networks.

At the generation level, back-to-back VSCs are needed as interfaces for distributed energy sources such as those used in wind energy conversion systems Fig. 1(a). At the transmission level, converter-based flexible ac transmission system (FACTS) controllers are employed to improve system stability and control power flow. A good example is the unified power-flow controller (UPFC) as shown in Fig. 1(b). At the distribution level, converter-based custom power controllers, such as shunt active filters Fig. 1(c), are used to improve power quality.

In terms of formulating the FCM of the VSC, the harmonic injections caused by external networks in Fig. 1 can all be modeled as ac-side voltage, and dc-side current harmonic sources at the points of common coupling. Fig. 2 shows the equivalent system.

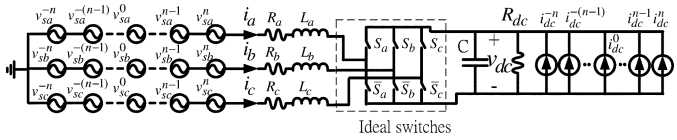

Fig. 3. Schematic diagram of a VSC with its ac and dc stimuli.

For a given set of switching times, the input ac voltage and dc current harmonics are linked to the output ac current and dc voltage harmonics via a frequency coupling matrix

$$\begin{bmatrix} I_a \\ I_b \\ I_c \\ V_{\rm dc} \end{bmatrix} = [\mathrm{FCM}] \begin{bmatrix} V_{sa} \\ V_{sb} \\ V_{sc} \\ I_{\rm dc} \end{bmatrix}. \tag{2}$$

In the frequency domain, the FCM of the VSC [3], [12], [17]–[19] is obtained via the following equations:

$$V_{sa} = \mathrm{SF}_a \otimes V_{\rm dc} \tag{3}$$
$$V_{sb} = \mathrm{SF}_b \otimes V_{\rm dc} \tag{4}$$
$$V_{sc} = \mathrm{SF}_a \otimes V_{\rm dc} \tag{5}$$
$$I_{\rm dc} = \mathrm{SF}_a \otimes I_a + \mathrm{SF}_b \otimes I_b + \mathrm{SF}_c \otimes I_c \tag{6}$$

where $\otimes$ represents the convolution operation, and SF_a, SF_b, SF_c are the switching functions of phase a, b, and c, respectively. Due to the nature of convolution process, the frequency-domain method inevitably suffers from truncation errors.

Therefore, the objective of this paper is to accurately and efficiently obtain the FCM in (2) from first principles (i.e., solving for piecewise LTI differential equations) in the time domain.

III. VSC Differential Equations

To construct an FCM of the VSC, Fig. 3 is considered. In the figure, there are $(2n+1)$ ac voltage and $(2n+1)$ dc current stimuli applied to the VSC. The stimuli are assumed to take the form $A_k e^{j(k\omega t+\theta_k)}$, where $k = -n, -(n-1), \ldots 0, \ldots, n-1$ and $n = \text{integer}$.

If the IGBT or GTO switches are assumed to be ideal, only the switching functions S_a, S_b, and S_c of the upper legs are needed for modeling the VSC. Consequently, the differential equations (see Appendix A for derivations) describing (3) are

$$\frac{d}{dt}\begin{bmatrix} \mathbf{x} \\ \mathbf{z} \end{bmatrix} = \begin{bmatrix} \mathbf{A}_{S_aS_bS_c} & \mathbf{N} \\ \mathbf{0} & \mathbf{\Omega} \end{bmatrix} \begin{bmatrix} \mathbf{x} \\ \mathbf{z} \end{bmatrix} \tag{7}$$

where

$$\mathbf{x} = [\, i_a \quad i_b \quad i_c \quad v_{\rm dc} \,]^T$$
$$\mathbf{z} = [\, \mathbf{v}_{sa} \quad \mathbf{v}_{sb} \quad \mathbf{v}_{sc} \quad \mathbf{i}_{\rm dc} \,]^T$$
$$\mathbf{A}_{S_aS_bS_c} = \begin{bmatrix} -\frac{R_{aa}}{L_t} & -\frac{R_{ab}}{L_t} & -\frac{R_{ac}}{L_t} & \frac{S'_a}{L_t} \\ -\frac{R_{ba}}{L_t} & -\frac{R_{bb}}{L_t} & -\frac{R_{bc}}{L_t} & \frac{S'_b}{L_t} \\ -\frac{R_{ca}}{L_t} & -\frac{R_{ca}}{L_t} & -\frac{R_{cc}}{L_t} & \frac{S'_c}{L_t} \\ \frac{S_a}{C} & \frac{S_b}{C} & \frac{S_c}{C} & \frac{-1}{R_{\rm dc}C} \end{bmatrix}$$

$$\mathbf{N}=\begin{bmatrix}\mathbf{N}_{aa} & \mathbf{N}_{ab} & \mathbf{N}_{\rm ac} & \mathbf{0}\\ \mathbf{N}_{ba} & \mathbf{N}_{bb} & \mathbf{N}_{bc} & \mathbf{0}\\ \mathbf{N}_{ca} & \mathbf{N}_{cb} & \mathbf{N}_{cc} & \mathbf{0}\\ \mathbf{0} & \mathbf{0} & \mathbf{0} & \mathbf{N}_l\end{bmatrix}$$

$$\mathbf{N}_{aa}=\left[\frac{L_b+L_c}{L_t}\quad \frac{L_b+L_c}{L_t}\quad \cdots\quad \frac{L_b+L_c}{L_t}\quad \cdots\quad \frac{L_b+L_c}{L_t}\quad \frac{L_b+L_c}{L_t}\right]$$

$$\mathbf{N}_{bb}=\left[\frac{L_a+L_c}{L_t}\quad \frac{L_a+L_c}{L_t}\quad \cdots\quad \frac{L_a+L_c}{L_t}\quad \cdots\quad \frac{L_a+L_c}{L_t}\quad \frac{L_a+L_c}{L_t}\right]$$

$$\mathbf{N}_{cc}=\left[\frac{L_a+L_b}{L_t}\quad \frac{L_a+L_b}{L_t}\quad \cdots\quad \frac{L_a+L_b}{L_t}\quad \cdots\quad \frac{L_a+L_b}{L_t}\quad \frac{L_a+L_b}{L_t}\right]$$

$$\mathbf{N}_{ab}=\left[-\frac{L_c}{L_t}\quad -\frac{L_c}{L_t}\quad \cdots\quad -\frac{L_c}{L_t}\quad \cdots\quad -\frac{L_c}{L_t}\quad -\frac{L_c}{L_t}\right]$$

$$\mathbf{N}_{\rm ac}=\left[-\frac{L_b}{L_t}\quad -\frac{L_b}{L_t}\quad \cdots\quad -\frac{L_b}{L_t}\quad \cdots\quad -\frac{L_b}{L_t}\quad -\frac{L_b}{L_t}\right]$$

$$\mathbf{N}_{bc}=\left[-\frac{L_a}{L_t}\quad -\frac{L_a}{L_t}\quad \cdots\quad -\frac{L_a}{L_t}\quad \cdots\quad -\frac{L_a}{L_t}\quad -\frac{L_a}{L_t}\right]$$

$$\mathbf{N}_{ba}=\mathbf{N}_{ab},\mathbf{N}_{ca}=\mathbf{N}_{\rm ac},\mathbf{N}_{cb}=\mathbf{N}_{bc}$$

$$\mathbf{N}_l=\left[\frac{1}{C}\quad \frac{1}{C}\quad \cdots\quad \frac{1}{C}\quad \cdots\quad \frac{1}{C}\quad \frac{1}{C}\right]$$

$$\mathbf{\Omega}=diag(\mathbf{\Omega}_1,\mathbf{\Omega}_1,\mathbf{\Omega}_1,\mathbf{\Omega}_1)$$

$$\mathbf{\Omega}_1=diag(-jn\omega,-j(n-1)\omega,\ldots,0,\ldots,j(n-1)\omega,jn\omega).$$

In the formulation just shown, the amplitudes (A_k) and phase angles (θ_k) of the ac and dc stimuli are uniquely related to the initial conditions $\mathbf{z}(\mathbf{0})$. In addition, although the switching functions S_a, S_b, and S_c are time varying, they are periodic with frequency ω. Hence, Fourier series coefficients exist for the steady-state solutions of (7).

IV. Augmenting Harmonic States to Differential Equations

The Fourier coefficients of any periodic signal $\psi(t)$ can be obtained by solving

$$\Psi_n=\frac{1}{T}\int_0^T\psi(t)e^{-jn\omega t}dt. \tag{8}$$

Consider the following differential equation:

$$\frac{dy}{dt}=my+h\psi(t) \tag{9}$$

whose solution is

$$y(T)=e^{mT}y(0)+\int_0^T e^{m(T-t)}h\psi(t)dt. \tag{10}$$

Comparing (4) and (6), one can immediately conclude that

$$\begin{aligned}y(T)&=\Psi_n\\ m&=jn\omega\\ h&=\frac{1}{T}e^{-jn\omega T}\end{aligned}$$

provided that $y(0)=0$.

Therefore, one can represent the harmonics of the interest by differential equation (9) [26]. Augmenting (9) to (7) yields

$$\frac{d}{dt}\hat{\mathbf{x}}=\hat{\mathbf{A}}\hat{\mathbf{x}} \tag{11}$$

where

$$\hat{\mathbf{x}}=\begin{bmatrix}\mathbf{x} & \mathbf{z} & \mathbf{y}\end{bmatrix}^T$$

$$\mathbf{y}=\begin{bmatrix}\mathbf{I_a} & \mathbf{I_b} & \mathbf{I_c} & \mathbf{V}_{\rm dc}\end{bmatrix}^T$$

$$\mathbf{I_a}=\begin{bmatrix}I_a^{-n} & I_a^{-(n-1)} & \cdots & I_a^0 & \cdots & I_a^{n-1} & I_a^n\end{bmatrix}^T$$

$$\mathbf{I_b}=\begin{bmatrix}I_b^{-n} & I_b^{-(n-1)} & \cdots & I_b^0 & \cdots & I_b^{n-1} & I_b^n\end{bmatrix}^T$$

$$\mathbf{I_c}=\begin{bmatrix}I_c^{-n} & I_c^{-(n-1)} & \cdots & I_c^0 & \cdots & I_c^{n-1} & I_c^n\end{bmatrix}^T$$

$$\mathbf{V}_{\rm dc}=\begin{bmatrix}V_{\rm dc}^{-n} & V_{\rm dc}^{-(n-1)} & \cdots & V_{\rm dc}^0 & \cdots & V_{\rm dc}^{n-1} & V_{\rm dc}^n\end{bmatrix}^T$$

$$\hat{\mathbf{A}}=\begin{bmatrix}\mathbf{A}_{S_aS_bS_c} & \mathbf{N} & \mathbf{0}\\ \mathbf{0} & \mathbf{\Omega} & \mathbf{0}\\ \mathbf{H} & \mathbf{0} & \mathbf{M}\end{bmatrix}$$

$$\mathbf{H}=\left[\begin{array}{cccc}\frac{e^{jn\omega T}}{T} & 0 & 0 & 0\\ \frac{e^{j(n-1)\omega T}}{T} & 0 & 0 & 0\\ \vdots & \vdots & \vdots & \vdots\\ \frac{1}{T} & 0 & 0 & 0\\ \vdots & \vdots & \vdots & \vdots\\ \frac{e^{-j(n-1)\omega T}}{T} & 0 & 0 & 0\\ \frac{e^{-jn\omega T}}{T} & 0 & 0 & 0\\ \hline 0 & \frac{e^{jn\omega T}}{T} & 0 & 0\\ 0 & \frac{e^{j(n-1)\omega T}}{T} & 0 & 0\\ \vdots & \vdots & \vdots & \vdots\\ 0 & \frac{1}{T} & 0 & 0\\ \vdots & \vdots & \vdots & \vdots\\ 0 & \frac{e^{-j(n-1)\omega T}}{T} & 0 & 0\\ 0 & \frac{e^{-jn\omega T}}{T} & 0 & 0\\ \hline 0 & 0 & \frac{e^{jn\omega T}}{T} & 0\\ 0 & 0 & \frac{e^{j(n-1)\omega T}}{T} & 0\\ \vdots & \vdots & \vdots & \vdots\\ 0 & 0 & \frac{1}{T} & 0\\ \vdots & \vdots & \vdots & \vdots\\ 0 & 0 & \frac{e^{-j(n-1)\omega T}}{T} & 0\\ 0 & 0 & \frac{e^{-jn\omega T}}{T} & 0\\ \hline 0 & 0 & 0 & \frac{e^{jn\omega T}}{T}\\ 0 & 0 & 0 & \frac{e^{j(n-1)\omega T}}{T}\\ \vdots & \vdots & \vdots & \vdots\\ 0 & 0 & 0 & \frac{1}{T}\\ \vdots & \vdots & \vdots & \vdots\\ 0 & 0 & 0 & \frac{e^{-j(n-1)\omega T}}{T}\\ 0 & 0 & 0 & \frac{e^{-jn\omega T}}{T}\end{array}\right]$$

$$\mathbf{M}=\mathrm{diag}(\mathbf{M}_1,\mathbf{M}_1,\mathbf{M}_1,\mathbf{M}_1)$$

$$\mathbf{M}_1=\mathrm{diag}(-jn\omega,-j(n-1)\omega,\ldots,0,\ldots,j(n-1)\omega,jn\omega).$$

V. Steady-State Analysis

Fig. 4 shows the typical pulse width modulated (PWM) switching functions of a VSC over one period T.

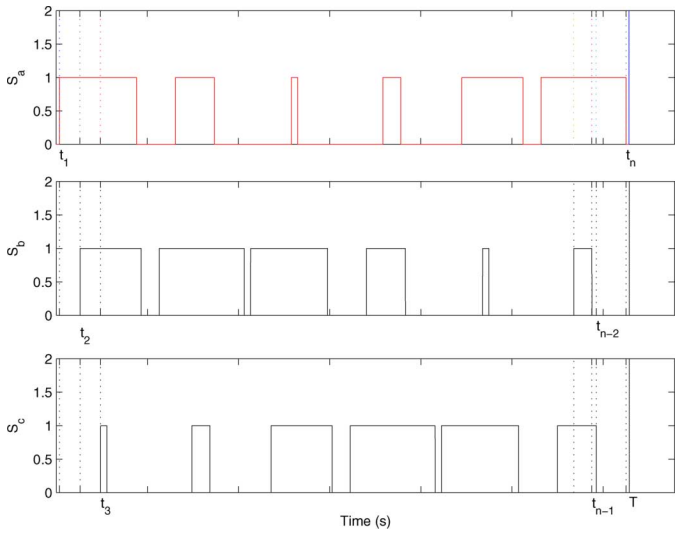

Fig. 4. Typical PWM switching function waveform.

For the given switching times (as in Fig. 4), the solutions of the states, $\mathbf{x}$, $\mathbf{y}$, and $\mathbf{z}$ over T is given by (12)

$$\hat{\mathbf{x}}(T) = \mathbf{\Phi}\hat{\mathbf{x}}(0) \tag{12}$$

where $\mathbf{\Phi} = e^{\hat{\mathbf{A}}_{t_{n+1}}(T-t_n)} \cdots e^{\hat{\mathbf{A}}_{t2}(t_2-t_1)} e^{\hat{\mathbf{A}}_{t_1}(t_1-0)}$, and $\hat{\mathbf{A}}_{t_k}$ represents $\hat{\mathbf{A}}$ between t_{k-1} and t_k. Fig. 5 shows the sparsity pattern of matrix $\hat{\mathbf{A}}$. As can be clearly noted, the matrix is very sparse, and is dominantly diagonal. Therefore, very little computation power is required to obtain $\mathbf{\Phi}$.

Central to the development of the FCM is that $\mathbf{\Phi}$ invariably has the following unique structure (see Appendix B for proof):

$$\begin{bmatrix} \mathbf{x}(T) \\ \mathbf{z}(T) \\ \mathbf{y}(T) \end{bmatrix} = \begin{bmatrix} \mathbf{A}_p & \mathbf{N}_p & \mathbf{0} \\ \mathbf{0} & \mathbf{\Omega}_p & \mathbf{0} \\ \mathbf{H}_p & \mathbf{Q}_p & \mathbf{M}_p \end{bmatrix} \begin{bmatrix} \mathbf{x}(0) \\ \mathbf{z}(0) \\ \mathbf{y}(0) \end{bmatrix}. \tag{13}$$

Several important relations may be extracted from (13). The first row of (13) contains the state trajectory over one period as a function of the initial conditions $\mathbf{z}(0)$

$$\mathbf{x}(T) = \mathbf{A}_p\mathbf{x}(0) + \mathbf{N}_p\mathbf{z}(0). \tag{14}$$

By assigning $\mathbf{y}(0) = \mathbf{0}$, the third row of (13) yields the solution to the Fourier integrals

$$\mathbf{y}(T) = \mathbf{H}_p\mathbf{x}(0) + \mathbf{Q}_p\mathbf{z}(0). \tag{15}$$

Applying the constraint $\mathbf{x}(T) = \mathbf{x}(0)$ to (14) yields the steady-state solution of the states, for given initial conditions $\mathbf{z}(0)$

$$\mathbf{x}(0) = (\mathbf{I} - \mathbf{A}_p)^{-1}\mathbf{N}_p\mathbf{z}(0). \tag{16}$$

Finally, the steady-state output harmonics are related to the initial conditions $\mathbf{z}(0)$ according to

$$\mathbf{y}(T) = \{\mathbf{H}_p[(\mathbf{I} - \mathbf{A}_p)^{-1}\mathbf{N}_p] + \mathbf{Q}_p\}\mathbf{z}(0). \tag{17}$$

VI. Frequency Coupling Matrix

Due to the fact that (17) relates the output harmonics to input initial conditions, a one-to-one relation between an input harmonic phasor and input initial conditions needs to be obtained in order to derive the FCM in (2).

As stated, stimuli take the form of $A_k e^{j(k\omega t+\theta_k)}$. Therefore, the initial condition for the stimulus' differential equations is simply equal to the harmonic phasor of that stimulus

$$\mathbf{z}(0) = \begin{bmatrix} V_a^{-n} \\ \vdots \\ V_a^{n} \\ V_b^{-n} \\ \vdots \\ V_b^{n} \\ V_c^{-n} \\ \vdots \\ V_c^{n} \\ I_{\mathrm{dc}}^{-n} \\ \vdots \\ I_{\mathrm{dc}}^{n} \end{bmatrix}.$$

Consequently, (17) directly relates input to output harmonics. This is explicitly shown in (18)

$$\begin{bmatrix} I_a^{-n} \\ \vdots \\ I_a^{n} \\ I_b^{-n} \\ \vdots \\ I_b^{n} \\ I_c^{-n} \\ \vdots \\ I_c^{n} \\ V_{\mathrm{dc}}^{-n} \\ \vdots \\ V_{\mathrm{dc}}^{n} \end{bmatrix} = [FCM] \begin{bmatrix} V_a^{-n} \\ \vdots \\ V_a^{n} \\ V_b^{-n} \\ \vdots \\ V_b^{n} \\ V_c^{-n} \\ \vdots \\ V_c^{n} \\ I_{\mathrm{dc}}^{-n} \\ \vdots \\ I_{\mathrm{dc}}^{n} \end{bmatrix} \tag{18}$$

where

$$[\mathbf{FCM}] = \{\mathbf{H}_p[(\mathbf{I} - \mathbf{A}_p)^{-1}\mathbf{N}_p] + \mathbf{Q}_p\}.$$

The following should be noted.

1) Equation (18) is a large-signal relation between input and output harmonics, as no linearization is required for its derivation.
2) The proposed method will be referred to as the "fast time-domain" method to distinguish from brute-force time-domain simulation.
3) Analytic expressions for $\mathbf{A}_p$, $\mathbf{N}_p$, $\mathbf{H}_p$, and $\mathbf{Q}_p$ are not required as these matrices may be extracted from the calculated $\mathbf{\Phi}$ matrix (see Appendix C for a sample Matlab code).
4) The proposed method only requires switching times to be known. Consequently, the FCMs of line-commutated converters can be found by the proposed method if the turnoff times of the diodes or thyristors are known. Usually,

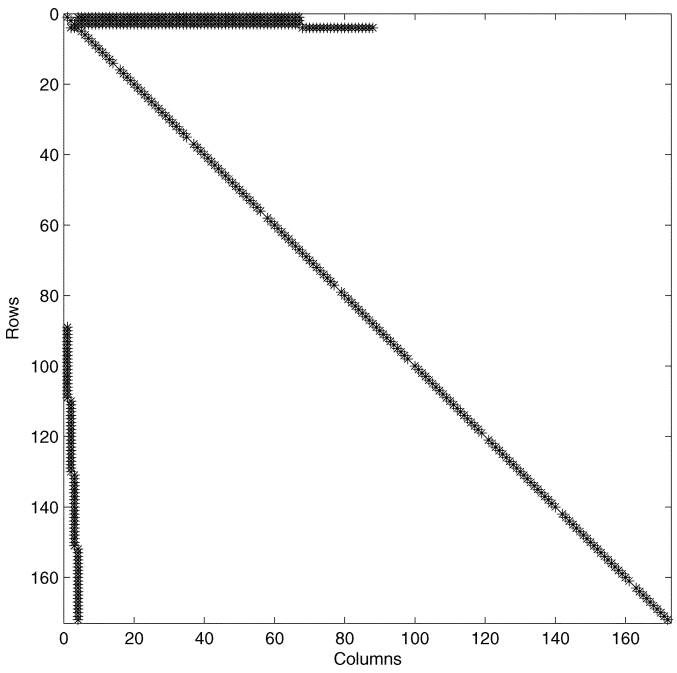

Fig. 5. Typical sparsity pattern of matrix $\hat{\mathbf{A}}$.

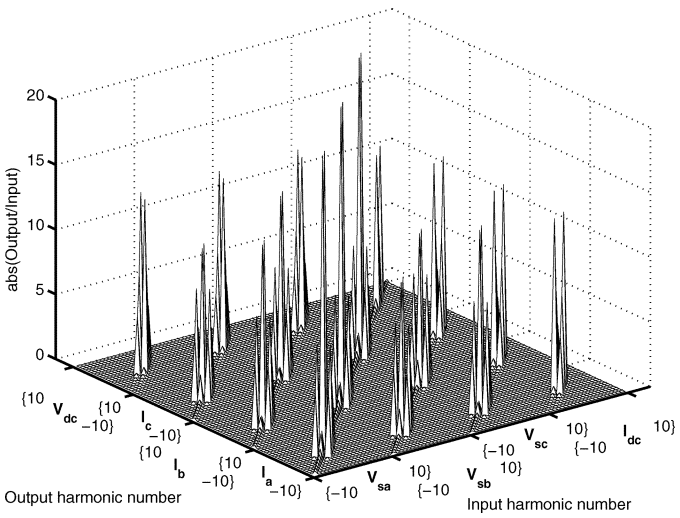

Fig. 6. FCM of a VSC with $m_f = \infty$ based on frequency-domain analysis under a balanced system parameter condition.

the turnoff times can be solved by a Newton–Raphson's method [23].

5) Since the stimuli have the form of $A_k e^{j(k\omega t+\theta_k)}$, it takes both positive and negative harmonics to constitute one sinusoid. This complex Fourier frequency domain is widely employed [3], [13], [14], [24], [25], [27] to analyze LTV systems because it only involves the multiplication of two infinite series to represent harmonic phasor convolution in the frequency domain [3]. Due to its popularity, this paper derives the FCM based on complex Fourier series.

6) An equivalent FCM may be derived based on the trigonometric Fourier series. In this case, the FCM needs to be expressed in terms of real numbers [18], [28] to relate input and output harmonics as in

$$\begin{bmatrix} \mathrm{Re}\{I_a^0\} \\ \mathrm{Im}\{I_a^0\} \\ \vdots \\ \mathrm{Re}\{I_a^n\} \\ \mathrm{Im}\{I_a^n\} \\ \mathrm{Re}\{I_b^0\} \\ \mathrm{Im}\{I_b^0\} \\ \vdots \\ \mathrm{Re}\{I_b^n\} \\ \mathrm{Im}\{I_b^n\} \\ \mathrm{Re}\{I_c^0\} \\ \mathrm{Im}\{I_c^0\} \\ \vdots \\ \mathrm{Re}\{I_c^n\} \\ \mathrm{Im}\{I_c^n\} \\ \mathrm{Re}\{V_{\mathrm{dc}}^0\} \\ \mathrm{Im}\{V_{\mathrm{dc}}^0\} \\ \vdots \\ \mathrm{Re}\{V_{\mathrm{dc}}^n\} \\ \mathrm{Im}\{V_{\mathrm{dc}}^n\} \end{bmatrix} = [FCM_{abc}] \begin{bmatrix} \mathrm{Re}\{V_a^0\} \\ \mathrm{Im}\{V_a^0\} \\ \vdots \\ \mathrm{Re}\{V_a^n\} \\ \mathrm{Im}\{V_a^n\} \\ \mathrm{Re}\{V_b^0\} \\ \mathrm{Im}\{V_b^0\} \\ \vdots \\ \mathrm{Re}\{V_b^n\} \\ \mathrm{Im}\{V_b^n\} \\ \mathrm{Re}\{V_c^0\} \\ \mathrm{Im}\{V_c^0\} \\ \vdots \\ \mathrm{Re}\{V_c^n\} \\ \mathrm{Im}\{V_c^n\} \\ \mathrm{Re}\{I_{\mathrm{dc}}^0\} \\ \mathrm{Im}\{I_{\mathrm{dc}}^0\} \\ \vdots \\ \mathrm{Re}\{I_{\mathrm{dc}}^n\} \\ \mathrm{Im}\{I_{\mathrm{dc}}^n\} \end{bmatrix}. \tag{19}$$

Two approaches to derive the real-valued FCM are listed in Appendix D.

VII. Example 1: m_f Very Large and Balanced System Parameters

The main limitation of frequency-domain analysis is that it suffers from truncation errors if insufficient harmonic terms are included in the calculation. The only case that the frequency domain does not suffer from this problem is when the ratio between switching and modulating frequency m_f is set to ∞. In this case, balanced switching functions can be simply represented as [29]

$$\begin{aligned} S_a &= \frac{m_a}{2}\cos(\omega t+\delta)+\frac{1}{2} \\ S_b &= \frac{m_a}{2}\cos\left(\omega t-\frac{2\pi}{3}+\delta\right)+\frac{1}{2} \\ S_c &= \frac{m_a}{2}\cos\left(\omega t-\frac{4\pi}{3}+\delta\right)+\frac{1}{2}. \end{aligned} \tag{20}$$

This case can serve as a benchmark to validate the derived FCM in the fast time-domain method when m_f of the fast time domain is set sufficiently large.

Figs. 6 and 7 show the absolute values of the FCM based on frequency domain (for $m_f = \infty$) and fast time-domain analysis (for $m_f = 111$) for harmonic numbers from -10 to 10. As can be seen, there is hardly any distinction between these two figures.

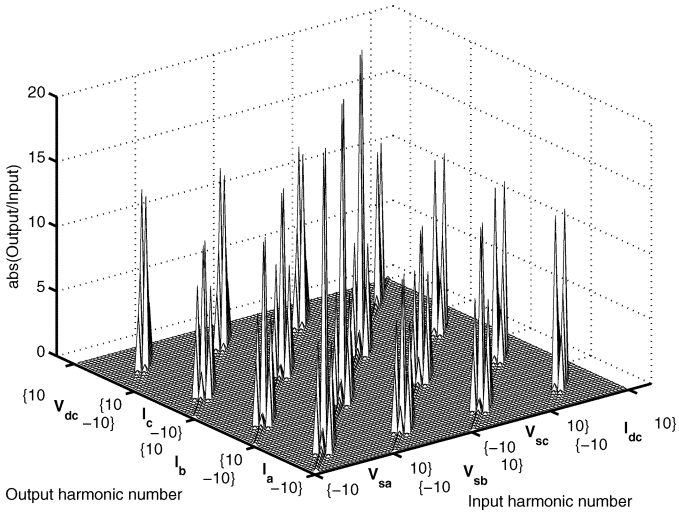

Fig. 7. FCM of a VSC with $m_f = 111$ based on fast time-domain analysis under a balanced system parameter condition.

TABLE I
TABLE OF PARAMETER LIST

Parameter list	$R_a = R_b = R_c = 0.02\Omega$ $L_a = L_b = L_c = 0.2H$ $C = 0.5F$, $\omega = 1rad/sec$ $m_a = 0.9$, $\delta = -1.2^\circ$ $R_{dc} = \infty$

TABLE II
TABLE OF INPUT STIMULI

Ac Input Stimuli	$V_{sa}^{-3} = 0.04V, V_{sa}^{3} = 0.04V$
	$V_{sa}^{-2} = 0.04V, V_{sa}^{2} = 0.04V$
	$V_{sa}^{-1} = 0.5V, V_{sa}^{1} = 0.5V$
	$V_{sb}^{-3} = -0.020 + j\frac{\sqrt{3}}{50}V, V_{sb}^{3} = -0.020 - j\frac{\sqrt{3}}{50}V$
	$V_{sb}^{-2} = -0.020 + j\frac{\sqrt{3}}{50}V, V_{sb}^{2} = -0.020 - j\frac{\sqrt{3}}{50}V$
	$V_{sb}^{-1} = -0.25 + j\frac{\sqrt{3}}{4}V, V_{sb}^{1} = -0.25 - j\frac{\sqrt{3}}{4}V$
	$V_{sc}^{-3} = -0.020 - j\frac{\sqrt{3}}{50}V, V_{sc}^{3} = -0.020 + j\frac{\sqrt{3}}{50}V$
	$V_{sc}^{-2} = -0.020 - j\frac{\sqrt{3}}{50}V, V_{sc}^{2} = -0.020 + j\frac{\sqrt{3}}{50}V$
	$V_{sc}^{-1} = -0.25 - j\frac{\sqrt{3}}{4}V, V_{sc}^{1} = -0.25 + j\frac{\sqrt{3}}{4}V$
Dc Input Stimuli	$I_{dc}^{0} = 0.05A$

Table I lists the normalized parameters being used in the simulation.

A sample set of the input stimuli, as given in Table II, is applied to the two FCMs. This allows the low-order harmonic voltages and currents produced by the two methods to be compared.

Fig. 8 shows the resulting ac current and dc voltage harmonics for frequency, fast time, and brute force time-domain (PSCAD/EMTDC) simulations. Good agreement among these three exists.

VIII. EXAMPLE 2: $m_f = 3$ AND BALANCED SYSTEM PARAMETERS

When m_f is reduced to 3, the errors due to harmonic truncation are apparent. Table III shows phase A current under the excitations of Table II when only harmonic numbers from -3 to 3 are included in the calculation. The discrepancies between

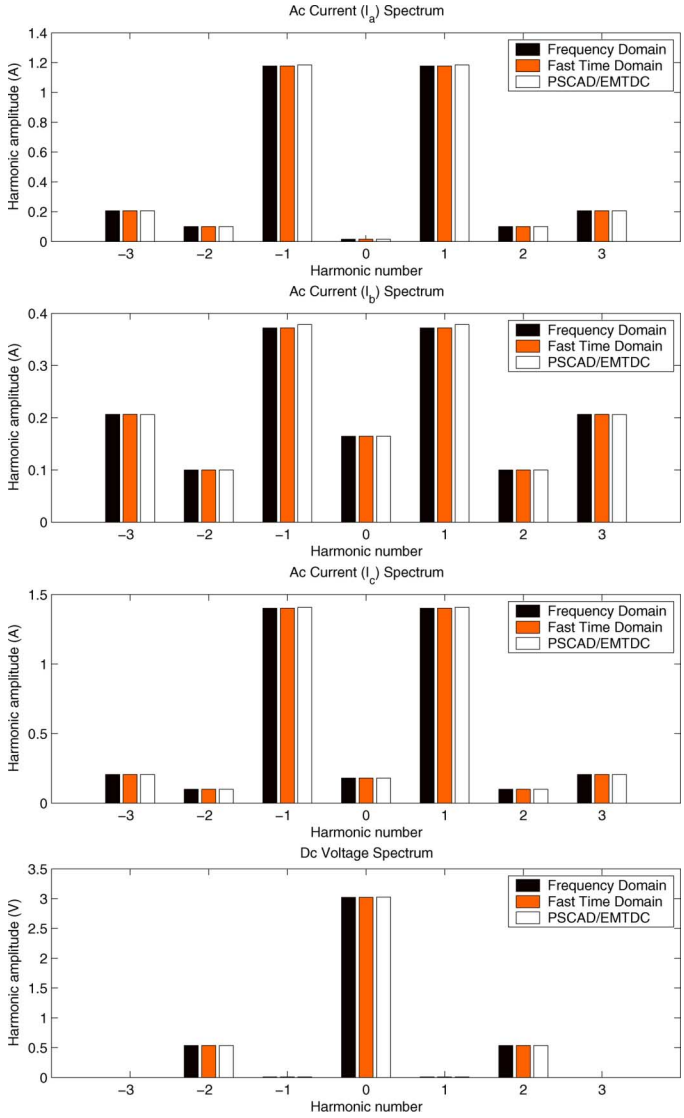

Fig. 8. Harmonic spectra under balanced system parameters and m_f is very large.

TABLE III
FIRST FOUR CURRENT HARMONICS FOR PHASE A WHEN $h = -3$ TO 3 UNDER BALANCED SYSTEM PARAMETER CONDITION

	Frequency domain	Fast time domain
I_a^{-3}	$0.0087 + j0.0237$	$0.0078 + j0.0244$
I_a^{-2}	$0.0101 + j0.1002$	$0.0096 + j0.0976$
I_a^{-1}	$-0.0169 - j0.6009$	$-0.0152 - j0.6152$
I_a^{0}	-0.0145	-0.0142
I_a^{1}	$-0.0169 + j0.6009$	$-0.0152 + j0.6152$
I_a^{2}	$0.0101 - j0.1002$	$0.0096 - j0.0976$
I_a^{3}	$0.0087 - j0.0237$	$0.0078 - j0.0244$

frequency domain and fast time domain are quite significant. As more harmonics are included in the frequency-domain calculation, frequency-domain results approach those of the fast time-domain solution. This fact can be observed from Table IV when harmonic numbers from -20 to 20 are included in the harmonic domain calculation. No truncation phenomenon exists with the fast time-domain solution.

TABLE IV
FIRST FOUR CURRENT HARMONICS FOR PHASE A WHEN $h = -20$ TO 20 UNDER BALANCED SYSTEM PARAMETER CONDITION

	Frequency domain	Fast time domain
I_a^{-3}	$0.0079 + j0.0245$	$0.0078 + j0.0244$
I_a^{-2}	$0.0099 + j0.0987$	$0.0096 + j0.0976$
I_a^{-1}	$-0.0154 - j0.6052$	$-0.0152 - j0.6152$
I_a^{0}	-0.0140	-0.0142
I_a^{1}	$-0.0154 + j0.6052$	$-0.0152 + j0.6152$
I_a^{2}	$0.0099 - j0.0987$	$0.0096 - j0.0976$
I_a^{3}	$0.0079 - j0.0245$	$0.0078 - j0.0244$

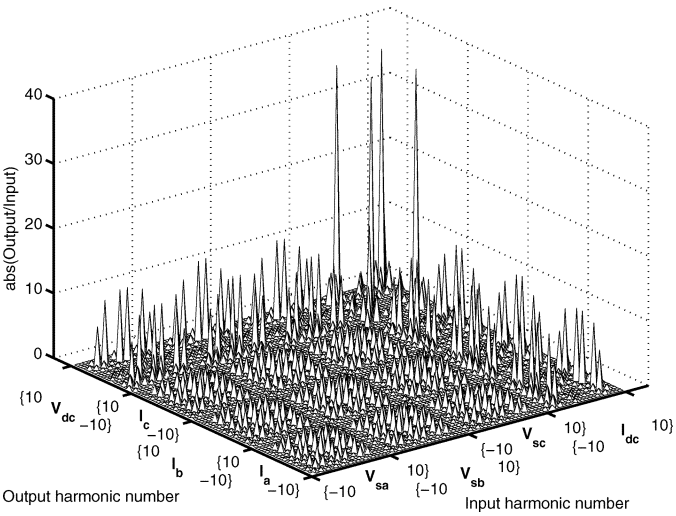

Fig. 9. FCM of a VSC with $m_f = 3$ based on frequency-domain analysis under an unbalanced system parameter condition.

IX. EXAMPLE 3: $m_f = 3$ AND UNBALANCED SYSTEM PARAMETERS

In this case, R_b, R_c, and L_b, L_c are kept the same as those used in the previous examples; however, R_a and L_a are increased by 10% to make the system unbalanced. In addition, the dc capacitance C is reduced to 0.05 F. The FCMs in the two domains are shown in Figs. 9 and 10, respectively, when harmonic numbers from −10 to 10 are included in the calculation. As can be noted in the figures, the FCMs differ because insufficient harmonic terms are included in the frequency domain. Consequently, when the sample set of input stimuli (see Table II) are applied to the resulting FCMs, the output currents differ significantly (Table V). Tables V–VII show the resulting phase A current for the first four harmonics. Once again, as the number of included harmonics increases, the frequency-domain results approach those of the fast time domain. However, 50 harmonic terms are needed in this case to obtain the same degree of accuracy as in the balanced case.

X. CONCLUSION

A time-domain-based method for calculating FCMs of power-electronic converters is presented. As an example, the method is employed to find the FCM of a VSC. The method is highly efficient compared with brute force time-domain simulation due to the sparse and mainly diagonal structure of the state matrix. In contrast to frequency-domain methods, the time-domain approach offers improved accuracy as it does not suffer from truncation errors. The derived FCM remains accurate regardless of the number of harmonic terms included during the calculation process. Therefore, the output of low-order harmonics will not be changed or "improved"

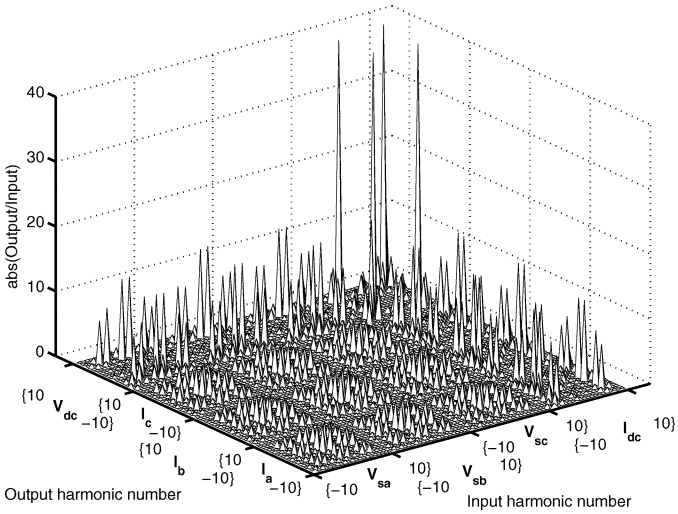

Fig. 10. FCM of a VSC with $m_f = 3$ based on fast time-domain analysis under an unbalanced system parameter condition.

TABLE V
FIRST FOUR CURRENT HARMONICS FOR PHASE A WHEN $h = -10$ TO 10 UNDER THE UNBALANCED SYSTEM PARAMETER CONDITION

	Frequency domain	Fast time domain
I_a^{-3}	$0.0153 + j0.0579$	$0.0168 + j0.0443$
I_a^{-2}	$0.0102 - j0.0329$	$0.0081 - j0.0126$
I_a^{-1}	$-0.0400 - j0.1828$	$-0.0385 - j0.1548$
I_a^{0}	-0.0147	-0.0127
I_a^{1}	$-0.0400 + j0.1828$	$-0.0385 + j0.1548$
I_a^{2}	$0.0102 + j0.0329$	$0.0081 + j0.0126$
I_a^{3}	$0.0153 - j0.0579$	$0.0168 - j0.0443$

TABLE VI
FIRST FOUR CURRENT HARMONICS FOR PHASE A WHEN $h = -25$ TO 25 UNDER THE UNBALANCED SYSTEM PARAMETER CONDITION

	Frequency domain	Fast time domain
I_a^{-3}	$0.0158 + j0.0436$	$0.0168 + j0.0443$
I_a^{-2}	$0.0086 - j0.0164$	$0.0081 - j0.0126$
I_a^{-1}	$-0.0379 - j0.1456$	$-0.0385 - j0.1548$
I_a^{0}	-0.0134	-0.0127
I_a^{1}	$-0.0379 + j0.1456$	$-0.0385 + j0.1548$
I_a^{2}	$0.0086 + j0.0164$	$0.0081 + j0.0126$
I_a^{3}	$0.0158 - j0.0436$	$0.0168 - j0.0443$

TABLE VII
FIRST FOUR CURRENT HARMONICS FOR PHASE A WHEN $h = -50$ TO 50 UNDER UNBALANCED SYSTEM PARAMETER CONDITION

	Frequency domain	Fast time domain
I_a^{-3}	$0.0169 + j0.0445$	$0.0168 + j0.0443$
I_a^{-2}	$0.0081 - j0.0130$	$0.0081 - j0.0126$
I_a^{-1}	$-0.0385 - j0.1519$	$-0.0385 - j0.1548$
I_a^{0}	-0.0128	-0.0127
I_a^{1}	$-0.0385 + j0.1519$	$-0.0385 + j0.1548$
I_a^{2}	$0.0081 + j0.0130$	$0.0081 + j0.0126$
I_a^{3}	$0.0169 - j0.0445$	$0.0168 - j0.0443$

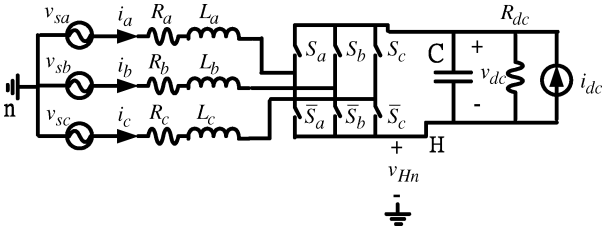

Fig. 11. Equivalent VSC's external networks.

when more high-order harmonic terms are included, as in the case of the frequency-domain methods.

Appendix A
Derivations of VSC Differential Equations

Fig. 11 shows the VSC circuit diagram where the floating dc node is denoted by H, and ground is denoted by n.

On the dc side

$$C\frac{dv_{\rm dc}}{dt} = S_a i_a + S_b i_b + S_c i_c - \frac{v_{\rm dc}}{R_{\rm dc}C} + i_{\rm dc}. \tag{21}$$

On the ac side

$$L_a\frac{di_a}{dt} = -(R_a)i_a - (v_{\rm dc}S_a + v_{Hn}) + v_{sa} \tag{22}$$

$$L_b\frac{di_b}{dt} = -(R_b)i_b - (v_{\rm dc}S_b + v_{Hn}) + v_{sb} \tag{23}$$

$$L_c\frac{di_c}{dt} = -(R_c)i_c - (v_{\rm dc}S_c + v_{Hn}) + v_{sc}. \tag{24}$$

Noting $i_a + i_b + i_c = 0$, (25) can be obtained by eliminating v_{Hn} in (22)–(24) via algebraic manipulation

$$\frac{d}{dt}\begin{bmatrix} i_a \\ i_b \\ i_c \\ v_{\rm dc}\end{bmatrix} = \begin{bmatrix} -\frac{R_{aa}}{L_t} & -\frac{R_{ab}}{L_t} & -\frac{R_{ac}}{L_t} & \frac{S'_a}{L_t} \\ -\frac{R_{ba}}{L_t} & -\frac{R_{bb}}{L_t} & -\frac{R_{bc}}{L_t} & \frac{S'_b}{L_t} \\ -\frac{R_{ca}}{L_t} & -\frac{R_{cb}}{L_t} & -\frac{R_{cc}}{L_t} & \frac{S'_c}{L_t} \\ \frac{S_a}{C} & \frac{S_b}{C} & \frac{S_c}{C} & \frac{-1}{R_{\rm dc}C}\end{bmatrix}\begin{bmatrix} i_a \\ i_b \\ i_c \\ v_{\rm dc}\end{bmatrix} + \begin{bmatrix} \frac{L_b+L_c}{L_t} & -\frac{L_c}{L_t} & -\frac{L_b}{L_t} & 0 \\ -\frac{L_c}{L_t} & \frac{L_a+L_c}{L_t} & -\frac{L_a}{L_t} & 0 \\ -\frac{L_b}{L_t} & -\frac{L_a}{L_t} & \frac{L_a+L_b}{L_t} & 0 \\ 0 & 0 & 0 & \frac{1}{C}\end{bmatrix}\begin{bmatrix} v_{sa} \\ v_{sb} \\ v_{sc} \\ i_{\rm dc}\end{bmatrix} \tag{25}$$

where $L_t = L_aL_b + L_bL_c + L_aL_c$, $R_{aa} = R_a(L_b + L_c) + R_bL_c$, $R_{ab} = 0$, $R_{ac} = (R_bL_c - R_cL_b)$, $R_{ba} = (R_cL_a - R_aL_c)$, $R_{bb} = R_b(L_a + L_c) + R_cL_a$, $R_{bc} = 0$, $R_{ca} = 0$, $R_{cb} = (R_aL_b - R_bL_a)$, $R_{cc} = R_c(L_a + L_b) + R_aL_b$, $S'_a = -(L_b + L_c)S_a + L_cS_b + L_bS_c$, $S'_b = -(L_a + L_c)S_b + L_cS_a + L_aS_c$, $S'_c = -(L_a + L_b)S_c + L_bS_a + L_aS_b$.

Note that (25) is not unique because one phase current is immediately known once the other two phase currents are known. Therefore, other legitimate representations exist. However, these representations all lead to one unique FCM.

Appendix B
Proof of Matrix Structure of $\hat{\Phi}$

The product of the two matrices $\hat{\mathbf{A}}_1$ and $\hat{\mathbf{A}}_2$

$$\begin{bmatrix} \mathbf{A}_1 & \mathbf{N} & \mathbf{0} \\ 0 & \mathbf{\Omega} & \mathbf{0} \\ \mathbf{H} & \mathbf{0} & \mathbf{M}\end{bmatrix}\begin{bmatrix} \mathbf{A}_2 & \mathbf{N} & \mathbf{0} \\ 0 & \mathbf{\Omega} & \mathbf{0} \\ \mathbf{H} & \mathbf{0} & \mathbf{M}\end{bmatrix} = \begin{bmatrix} \mathbf{A}_1\mathbf{A}_2 & \mathbf{A}_1\mathbf{N} + \mathbf{N}\mathbf{\Omega} & \mathbf{0} \\ \mathbf{0} & \mathbf{\Omega}^2 & \mathbf{0} \\ \mathbf{H}\mathbf{A}_2 + \mathbf{M}\mathbf{H} & \mathbf{H}\mathbf{N} & \mathbf{M}^2\end{bmatrix} = \begin{bmatrix} \boldsymbol{\alpha} & \boldsymbol{\beta} & \mathbf{0} \\ \mathbf{0} & \boldsymbol{\gamma} & \mathbf{0} \\ \boldsymbol{\eta} & \boldsymbol{\xi} & \boldsymbol{\varsigma}\end{bmatrix}. \tag{26}$$

Hence, $e^{\hat{\mathbf{A}}\mathbf{t}}$ also has the form of (26) because of the fact that

$$e^{\hat{\mathbf{A}}t} = I + \hat{\mathbf{A}}t + \frac{\hat{\mathbf{A}}^2t^2}{2!} + \frac{\hat{\mathbf{A}}^3t^3}{3!} + \cdots + \frac{\hat{\mathbf{A}}^nt^n}{n!}.$$

Appendix C
Sample Matlab Code for Obtaining FCM

User Input:

Switching times

$$tau_I = [0.0526; 0.5303; 0.9935; 1.0998; 1.5775; 2.0407; \ldots 2.1470; 2.6247; 3.0879; 3.1942; 3.6719; 4.1351; \ldots 4.2414; 4.7191; 5.1823; 5.2886; 5.7663; 6.2295].$$

Period $T = 2\pi$.

Switching sequences

$$S_a : Sseq_I(:,1) = [0;1;1;1;1;0;0;0;0;1;0;0;\ldots 0;0;1;1;1;1;0].$$

$$S_b : Sseq_I(:,2) = [0;0;1;1;1;1;0;1;1;1;1;0;\ldots 0;0;0;1;0;0;0].$$

$$S_c : Sseq_I(:,3) = [0;0;0;1;0;0;0;0;1;1;1;1;\ldots 0;1;1;1;1;0;0].$$

Matlab codes starts here

h = 3; Hh = −h : 1 : h.

%code the seq to integer number

Sdseq_I = Sseq_I(:, 1) ∗ 2^2 + Sseq_I(:, 2) ∗ 2^1 + ⋯

Sseq_I(:, 3) ∗ 2^0 + 1.

%8 possibilities

S_I = [000; 001; 010; 011; 100; 101; ….

110; 111].

h_l = length(Hh); len = 4 * length(Hh) + 4.

Ra = 0.02; Rb = Ra; Rc = Ra; La = 0.2; Lb = La; Lc = Lb; C = 0.5.

Lt = La * Lb + Lb * Lc + La * Lc.

Raa = (Ra*Lb+Ra*Lc+Rb*Lc); Rac = (Rb*Lc−Rc*Lb).

Rba = (Rc*La−Ra*Lc); Rbb = (Rb*La+Rb*Lc+Rc*La).

Rcb = (Ra*Lb−Rb*La); Rcc = (Rc*La+Rc*Lb+Ra*Lb).

%construct submatrices

N = [(Lb + Lc)/Lt * ones(1, h_l), −Lc/Lt * ones(1, h_l), ...

−Lb/Lt * ones(1, h_l), zeros(1, h_l); −Lc/Lt * ones(1, h_l), ...

(La + Lc)/Lt * ones(1, h_l), −La/Lt * ones(1, h_l), zeros(1, h_l); ....

−Lb/Lt * ones(1, h_l), −La/Lt * ones(1, h_l), ...

(La + Lb)/Lt * ones(1, h_l), zeros(1, h_l); ....

zeros(1, h_l), zeros(1, h_l), zeros(1, h_l), 1/C * ones(1, h_l)].

Omega = blkdiag(j * w * diag(Hh), j * w * diag(Hh), ...

j * w * diag(Hh), j * w * diag(Hh)).

M = blkdiag(j * w * diag(Hh), j * w * diag(Hh), ...

j * w * diag(Hh), j * w * diag(Hh)).

for k = 1 : length(Hh).

H(k, :) = [1/T * exp(−j * Hh(k) * w * T), zeros(1, len − 1)].

H(k + length(Hh), :) = [0, 1/T * exp(−j * Hh(k) * w * T). ....

zeros(1, len − 2)].

H(k+2 *length(Hh), :) = [0, 0, 1/T*exp(−j*Hh(k)*w*T), ...

zeros(1, len − 3)].

H(k+3*length(Hh), :) = [0, 0, 0, 1/T*exp(−j*Hh(k)*w*T), ...

zeros(1, len − 4)]

end

for i = 1 : 8 %construct A hat

A_hat(:, :, i) = [[[−Raa/(Lt), 0, −Rac/Lt, ...

−S_I(i, 1) *(Lb+Lc)/Lt+S_I(i, 2)*Lc/Lt+S_I(i, 3)*Lb/Lt.

−Rba/Lt, −Rbb/Lt, 0, Lc/Lt * S_I(i, 1) − (La + Lc)/Lt * S_I(i, 2) + ⋯.

La/Lt * S_I(i, 3); 0, −Rcb/Lt, −Rcc/Lt, −(La + Lb)/Lt * S_I(i, 3) + ⋯.

La/Lt * S_I(i, 2) + Lb/Lt * S_I(i, 1); S_I(i, 1)/C, S_I(i, 2)/C, ...

S_I(i, 3)/C, −1/(R_dc*C)], N; zeros(4*(length(Hh)), 4), ...

Omega], zeros(len, 4 * length(Hh)); H, M]

end

tau = [tau_I; T].

PHI = expm(A_hat(:, :, Sdseq_I(1)) * tau(1)).

for i = 2 : length(tau).

PHI = expm(A_hat(:, :, Sdseq_I(i)) * ⋯.

(tau(i) − tau(i − 1))) * PHI

end

Ap = PHI(1 : 4, 1 : 4); %access to submatrices to get FCM.

Np = PHI(1 : 4, 5 : len); Hp = PHI(len + 1 : length(PHI), 1 : 4).

Qp = PHI(len + 1 : size(PHI), 5 : len).

FCM = Hp * (inv(eye(4) − Ap)) * Np + Qp; %Get the resulting FCM.

Appendix D
Real-Valued FCM

First Approach: The real-valued FCM can be directly derived from the complex FCM of (18). To demonstrate this fact, consider the following complex FCM:

$$\begin{bmatrix} I_a^{-1} \\ I_a^1 \end{bmatrix} = \begin{bmatrix} Y_{11} & Y_{12} \\ Y_{21} & Y_{22} \end{bmatrix} \begin{bmatrix} V_a^{-1} \\ V_a^1 \end{bmatrix}. \tag{27}$$

Thus, I_a^1 can be expressed as

$$I_a^1 = Y_{21} V_a^{-1} + Y_{22} V_a^1 \tag{28}$$

where $Y_{21} = Y_{21R} + jY_{21I}$, $Y_{22} = Y_{22R} + jY_{22I}$, $I_a^1 = I_{aR}^1 + jI_{aI}^1$, and $V_a^1 = V_{aR}^1 + jV_{aI}^1$.

Noting that $V_a^{-1} = V_a^*$, one can turn the complex FCM into the real-valued FCM [28]

$$\begin{bmatrix} I_{aR}^1 \\ I_{aI}^1 \end{bmatrix} = \begin{bmatrix} Y_{21R} + Y_{22R} & Y_{22I} - Y_{21I} \\ Y_{21I} + Y_{22I} & Y_{21R} - Y_{22R} \end{bmatrix} \begin{bmatrix} V_{aR}^1 \\ V_{aI}^1 \end{bmatrix}. \tag{29}$$

Apply (29) to each harmonic coupling term in (18), one can convert (18) into (19).

Note that due to the phase dependence of the converters [28], in general, the FCM in (29) does not have the form of

$$\begin{bmatrix} p & -q \\ q & p \end{bmatrix}; p, q \in R$$

as is the case for LTI components.

Second Approach: If one chooses the input stimuli to have the form of $A_k \cos(k\omega t + \theta_k)$ or $A_k \sin(k\omega t + \theta_k)$ where $k = 0, 1, \ldots, n \in Z$, then the stimuli can be easily augmented to the state matrix by modeling them as harmonic oscillators [30] as

$$\frac{d}{dt} \begin{bmatrix} z_{ax}^k \\ z_{ay}^k \end{bmatrix} = \begin{bmatrix} 0 & -k\omega \\ k\omega & 0 \end{bmatrix} \begin{bmatrix} z_{ax}^k \\ z_{ay}^k \end{bmatrix}. \tag{30}$$

However, the FCM in this case can only take real values because an one-to-one relation exists between input harmonics (complex numbers) and input initial conditions (real numbers) only when input harmonics are broken into real and imaginary parts.

For instance, if $v_{sa}^k = A_k \cos(k\omega t + \theta_k)$

$$\begin{bmatrix} \mathrm{Re}\{V_{sa}^k\} \\ \mathrm{Im}\{V_{sa}^k\} \end{bmatrix} = \begin{bmatrix} A_k \cos(\theta_k) \\ A_k \sin(\theta_k) \end{bmatrix} = \begin{bmatrix} z_{ax}^k(0) \\ z_{ay}^k(0) \end{bmatrix}. \quad (31)$$

REFERENCES

[1] "Task force on harmonics modeling and simulation, "Modeling and simulation of the propagation of harmonics in electric power networks–Part I: Concepts, models and simulation techniques"," *IEEE Trans. Power Del.*, vol. 11, no. 1, pp. 452–465, Jan. 1996.

[2] B. C. Smith, J. Arrillaga, A. R. Wood, and N. R. Watson, "A review of iterative harmonic analysis for ac-dc power systems," *IEEE Trans. Power Del.*, vol. 13, no. 1, pp. 180–185, Jan. 1998.

[3] E. Acha and M. Medina, *Power Systems Harmonics: Computer Modeling and Analysis*. New York: Wiley, 2001.

[4] E. Larsen, D. Baker, and J. McIver, "Low-order harmonic interactions on AC/DC systems," *IEEE Trans. Power Del.*, vol. 4, no. 1, pp. 493–501, Jan. 1989.

[5] S. G. Jalali and R. H. Lasseter, "Harmonic interaction of power system with static switching circuits," in *Proc. IEEE Ind. Appl. Soc. Annu. Meeting*, 1991, pp. 330–337.

[6] N. Rajagopal and J. E. Quaicoe, "Harmonic analysis of three-phase AC/DC converters using the harmonic admittance method," in *Proc. Canadian Conf. Electrical and Computer Engineering*, Sep. 14–17, 1993, pp. 313–316.

[7] M. Fauri, "Harmonic modelling of non-linear load by means of crossed frequency admittance matrix," *IEEE Trans. Power Syst.*, vol. 12, no. 4, pp. 1632–1638, Nov. 2001.

[8] Ä. Ekström, "Calculation of transfer functions for a forced-commutated voltage-source converter," in *Proc. 22nd Annu. IEEE Power Electronics Specialists Conf.*, Jun. 1991, pp. 314–322.

[9] R. W. Erickson and D. Maksimović, *Fundamentals of Power Electronics*, 2nd ed. Norwell, MA: Kluwer, 2001.

[10] C. Schauder and H. Mehta, "Vector analysis and control of advanced static var compensators," *Proc. Inst. Elect. Eng. C*, vol. 140, no. 4, pp. 299–306, Jul. 1993.

[11] D. Shen, Z. Wang, J. Y. Chen, and Y. H. Song, "Harmonic resonance phenomena in STATCOM and relationship to parameters selection of passive components," *IEEE Trans. Power Del.*, vol. 16, no. 1, pp. 46–52, Jan. 2001.

[12] M. Mohaddes, A. Gole, and S. Elez, "Steady state frequency response of STATCOM," *IEEE Trans. Power Del.*, vol. 16, no. 1, pp. 18–23, Jan. 2001.

[13] T. Noda, A. Semlyen, and R. Iravani, "Harmonic domain dynamic transfer function of nonlinear time-periodic network," *IEEE Trans. Power Del.*, vol. 18, no. 4, pp. 1433–1441, Oct. 2003.

[14] E. Möllerstedt and B. Bernhardsson, "Out of control because of harmonics– An analysis of the harmonic response of an inverter locomotive," *IEEE Control Syst. Mag.*, pp. 70–81, Aug. 2000.

[15] A. C. Pradhan and P. W. Lehn, "Frequency domain analysis of static synchronous series compensator," *IEEE Trans. Power Del.*, vol. 21, no. 1, pp. 440–449, Jan. 2006.

[16] A. Wood and C. M. Osauskas, "A linear frequency-domain model of a STATCOM," *IEEE Trans. Power Del.*, vol. 19, no. 3, pp. 1410–1418, Jul. 2004.

[17] R. Carbone, A. Lo Schiavo, P. Marino, and A. Testa, "A new method based on periodic convolution for sensitivity analysis of multi-stage conversion systems," in *Proc. 9th Int. Conf. Harmonics and Quality of Power*, Oct. 1– 4, 2000, vol. 1, pp. 69–74.

[18] C. Saniter, A. R. Wood, R. Hanitsch, and D. Schulz, "Modelling the effects of ac system impedance unbalnce on PWM converters using frequency couplig matrices," in *Proc. IEEE Bologna PowerTech Conf.*, Jun. 23– 26, 2003.

[19] C. D. Collins, G. N. Bathurst, N. R. Watson, and A. R. Wood, "Harmonic domain approach to STATCOM modelling," *Proc. Inst. Elect. Eng., Gen., Transm. Distrib.*, vol. 152, no. 2, pp. 194–200, Mar. 2005.

[20] L. Hu and R. Yacamini, "Harmonic transfer through converters and HVDC links," *IEEE Trans. Power Electron.*, vol. 7, no. 3, pp. 514–525, Jul. 1992.

[21] P. Wood, *Switching Power Converters*. New York: Van Nostrand, 1981.

[22] H. S. Black, *Modulation Theory*. New York: Van Nostrand, 1953.

[23] B. K. Perkins and M. R. Iravani, "Novel calculation of HVDC converter by linearization in the time domain," *IEEE Trans. Power Del.*, vol. 12, no. 2, pp. 867–873, Apr. 1997.

[24] N. M. Wereley, "Analysis and control of linear periodically time varying system," Ph.D. dissertation, Dept. Aeronautics Astronautics, Mass. Inst. Technol., Cambridge, MA, 1991.

[25] P. Vanassche, G. Gielen, and W. Sansen, "Symbolic modeling of peridocially time-varing systems using harmonic transfer matrices," *IEEE Trans. Comput. Aided Design*, vol. 21, no. 9, pp. 1011–1024, Sep. 2002.

[26] P. W. Lehn, "Direct harmonic analysis of the voltage source converter," *IEEE Trans. Power Del.*, vol. 18, no. 3, pp. 1304–1042, Jul. 2003.

[27] A. Semlyen, J. F. Eggleston, and A. Arrillaga, "Admittance matrix model of a synchronous machine for harmonic analysis," *IEEE Trans. Power Syst.*, vol. PWRS-2, no. 4, pp. 833–840, Nov. 1987.

[28] J. Arrillaga, B. C. Smith, N. R. Watson, and A. Wood, *Power Systems Harmonics Analysis*. New York: Wiley, 1997.

[29] P. T. Krein, *Elements of Power Electronics*. New York: Oxford Univ. Press, 1998.

[30] P. W. Lehn, "Exact modeling of the voltage source converter," *IEEE Trans. Power Del.*, vol. 17, no. 1, pp. 217–222, Jan. 2002.

P. W. Lehn (SM'05) received the B.Sc. and M.Sc. degrees in electrical engineering from the University of Manitoba, Winnipeg, MB, Canada, in 1990 and 1992, respectively, and the Ph.D. degree from the University of Toronto, Toronto, ON, Canada, in 1999.

From 1992 to 1994, he was with the Network Planning Group of Siemens AG, Erlangen, Germany. Currently, he is an Associate Professor at the University of Toronto. His research interests include analytical modeling of nonlinear and switched circuits.

K. L. Lian (S'03) received the B.A.Sc. (Hons.) and M.A.Sc. degrees in electrical engineering from the University of Toronto, Toronto, ON, Canada, in 2001 and 2003, respectively, where he is currently pursuing the Ph.D. degree.